

Synergistic influence of molybdate ions with TDMTAA on corrosion inhibition of ordinary steel in cooling water system

M. Cenoui, N. Dkhireche, O. Kassou, M. Ebn Touhami, R. Tourir*, A. Dermaj, N. Hajjaji

Laboratory of Electrochemistry, Corrosion and Environment, Faculty of Science, B.P. 133-14000 Kenitra, Morocco.

* Corresponding author: Tel.: + 212 670 52 69 59; Fax: + 212 537 36 27 32. E-mail address: tourir8@yahoo.fr
Received in 13 Aug 2010, Revised 25 Sept, Accepted 26 Sept 2010.

Abstract

This work was carried out to study the inhibition of corrosion of ordinary steel in cooling water system solution by a multi-component. The inhibitive formulation was composed of 2- (2-thio-dodecyl-5-methyl-1,3,4-triazol)yl acetic acid (TDMTAA) associated with molybdate ions. The obtained results lead that TDMTAA inhibits the corrosion of ordinary steel in the considered medium. The corresponding inhibition efficiency increases by increases by inhibitor concentration and also by adding of molybdate ions. The values of the synergism parameter (S_0) indicate that the enhanced inhibition efficiency in the presence of molybdate ions is only due to synergism and there is a definite contribution from the inhibitor molecule, which are adsorbed by coulombic interaction on metallic surface, where molybdate ions are already adsorbed and thus reduce the corrosion rate. The inhibition efficiency of mixture increases by increasing of temperature, pH and immersion time and leads a maximum of 99%.

Keywords: Inhibition corrosion, TDMTAA, Molybdate, Synergistic, Ordinary steel, Cooling water system.

1. Introduction

Natural water is frequently used in cooling systems. This use needs in especially cases treatments to minimise the corrosion of processes metals. Open recirculating cooling water systems that reuse cooling water are frequently used at large central utility stations, at chemical, petrochemical, and petroleum refining plants, in steel and paper mills, and at all types of processing plants [1]. Open recirculation cooling water systems continuously reuse the water that go through the heat transfer equipment.

If absolutely pure water was used in the cooling system, none of the problems would exist. Unfortunately, waters contain dissolved and suspended solids, dissolved and suspended organic matters, and dissolved gases [2]. Finally, the open recirculating system, with longer holding times at higher temperatures in the presence of higher dissolved solids concentrations, produces more severe corrosion, scaling and microbiological growth [2]. These problems can occur jointly, reducing the thermal efficiency of the circuit with significant economic repercussions.

Many inhibitors have been used in cooling water systems in order to reduce or eliminate these problems [3-9]. Particularly, fatty amines associated with phosphonocarboxylic acid salts, hydroxyethane diphosphonic acid (HEDP) and hydroxyphosphonoacetic acid (HPA) were the standard corrosion inhibitors [10, 11]. Other authors used other inhibitors such as triazole and its derivatives associated with cetyl trimethyl ammonium bromide (CTAB) or with isothiazolone in order to kill micro-organismes [12, 13].

The cost of inorganic inhibitors is low, but most are toxic e.g., chromate, mercuride, nitrite, arsenate etc. [14]. As an environmentally acceptable and effective corrosion inhibitor for zinc, galvanized steel, and other metals, molybdate ion (MoO_4^{2-}) has been widely investigated in a variety of corrosive media [15-17]. Many other researchers have concentrated on the synergetic effect between molybdate ions and other organic and inorganic compounds for corrosion reduction in cooling water systems [18-22]. Different operational parameters such as cooling water pH, inhibitor concentration, water circulation velocity and the concentration of the other ions present in water may have a considerable influence on molybdate inhibition efficiency in cooling waters [23, 24].

In this paper we have studied the effect of an environmentally acceptable multi-component inhibitor that would simultaneously inhibit corrosion and microorganisms. A preliminary series of laboratory experiments was carried out in cooling water containing different inhibitor (mixture of TDMTAA, molybdate and biocides) from which the most promising mixture was selected for subsequent testing.

2. Experimental procedure

2.1. Synthesis of the TDMTAA Compound

TDMTAA has been prepared by a new method developed in our laboratory. This surfactant compound was improved by solid-liquid phase transfer catalysis method [25]. Moreover this product has been purified and characterised by NMR ^1H , NMR ^{13}C , masse and elemental analysis.

We have reacted the 5-dodecyl-3-methyl-1,2,4-triazole-5-thione with the bromoacetic acid. This leads us to obtain a monocatener surfactant that the polar head contain an acidic function. The synthesised compound has been obtained with good yield (- yield : 80 %; mp: 76-80 °C) and has two isomer which presented in figure 1. The ^1H NMR and ^{13}C NMR spectral data of the product are as follows:

- ^1H NMR (CDCl_3 ; 300MHZ) : 1.04 -1.8 ppm (m,50H, $2(\text{CH}_2)_{11}\text{-CH}_3$); 2.43 ppm (s, 3H, CH_3); 2.50 ppm (s, 3H, CH_3), 3.17(t,2H, $\text{CH}_2\alpha\text{S}$), 3.26(t,2H, $\text{CH}_2\alpha\text{S}$), 4.72 ppm (s, 2H, $\text{CH}_2\alpha\text{C=O}$), 4.77 ppm (s, 2H, $\text{CH}_2\alpha\text{C=O}$).

- ^{13}C NMR (CDCl_3 ; 75.47 MHZ):

* Alkyl Chain: 11.88, 22.78, 29.09, 29.41, 29.51, 29.83, 29.89, 32.04, 33.43.

* 1,2,4-triazole :13.80 and 14.08 (2CH_3); 153.16 and 154.74 (2C_3); 158.45 and 160.56 (2C_5)

* Two C=O : 173.09 and 173.4 ppm.

* The CH_2 at α of C=O: 51.73 and 52 ppm.

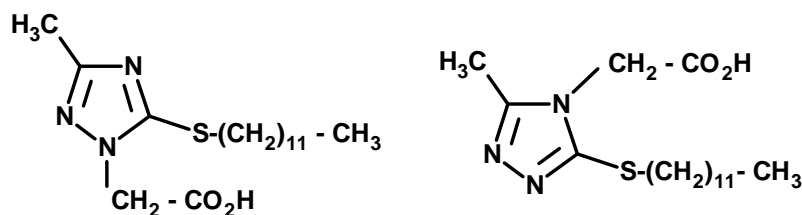


Figure 1. Structure of 2- (2-thio-dodecyl-5-methyl-1,3,4-triazol)yl acetic acid (two isomer)

2.2. Formulation of inhibitor

In accordance with the numerous works improved in our laboratory using the surfactants compounds to polar head 1,2,4-triazole like corrosion inhibitors [26, 27], we were interested in this work in the study of the effect of 2-(2-thio-dodecyl-5-methyl-1,3,4-triazol)yl acetic acid (TDMTAA) on corrosion of ordinary steel in cooling water system.

In order to minimise corrosion, scale and microbial problems, this new inhibitor for cooling water systems was developed. The inhibitor formulation was blended from TDMTAA and molybdate. The selection of this composition was based on screening tests of various concentrations of the compounds and their blends.

2.3. Metallic samples

The specimens were cut from commercial ordinary steel its chemical composition is (in wt.%): C-0.11, Si-0.24, Mn-0.47, Cr-0.12, Mo-0.02, Ni-0.1, Al-0.03, Cu-0.14, W-0.06, Co<0.0012, V<0.003 and the remainder iron was used as the substrate. Before each experiment, the electrode was polished using emery papers until 1200 grade, after this, the electrode was cleaned with distilled water, degreased in acetone before use and dried with hot air.

2.4. Experimental conditions

The temperature of the cooling water was adjusted to 32 ± 1 °C and its pH is 7.5, respectively. Table 1 gives the chemical composition of cooling water system. This natural solution is characterized by its low conductivity and its corrosive character.

Table 1: Chemical composition of cooling water system used.

Elements	Mg^{2+}	Cl^-	Ca^{2+}	SO_4^{2-}	HCO_3^-	TDS	σ ($\mu\text{s}/\text{cm}$)
Concentration (ppm)	235	414	100	145	220	898	1426

2.5. Electrochemical tests

Electrochemical measurements were conducted in a conventional three-electrode thermostated cell. A platinum disc was used as counter electrode and a saturated calomel electrode (sce) as reference electrode. The working electrode was an ordinary steel disc. The specimens were machined into cylinders and mounted in polytetrafluoroethylene (PTFE) moulds. The area in contact with the corrosive solution was 1 cm².

The working electrode was immersed in the test solution during 1 h until a steady-state open circuit potential (E_{ocp}) was obtained. The cathodic polarization curve was recorded by polarization from E_{ocp} to negative direction under potentiodynamic conditions corresponding to 1 mV.s⁻¹ vs SCE (sweep rate) and under air atmosphere. After this scan, the anodic polarization curve was recorded by polarization from the E_{ocp} to positive direction. The potentiodynamic measurements were carried out using a Potentiostat type, VoltaLab PGZ 100, controlled by a personal computer. Since the conductivity of medium studied is low, the polarization curves J(E) were corrected from ohmic drop; that is, by R_s×J. The solution resistance, R_s, was determined by the electrochemical impedance spectroscopy. On the Nyquist diagrams, R_s is the abscissa of high-frequency intersection of the diagram with the real axis.

The evaluation of corrosion kinetics parameters was obtained using a fitting by Stern–Geary equation. The inhibition efficiency was evaluated from the measured J_{corr} values using the relationship:

$$IE\% = \left(1 - \frac{j_{corr}}{j_{corr}^0} \right) \times 100 \quad (1)$$

The degree of surface coverage (θ) and the inhibition efficiency IE% were calculated from the following equations:

$$\theta = 1 - \frac{j_{corr}}{j_{corr}^0} \quad (2)$$

Where j_{corr}⁰ and j_{corr} are the corrosion current values without and with the addition of various concentration of inhibitor.

2.6. Scanning electron microscopy (SEM)

The surfaces (2cm×1cm×0.4cm) of ordinary steel immersed for 2 days in cooling water system, without and with the inhibitor formulation, were analyzed by scanning electronic microscope JOEL JSM-5500 type.

3. Results and discussion

3.1. Electrochemical tests

Effect of TDMTAA concentration

Polarization curves of ordinary steel in cooling water system in the absence and presence of different concentrations of TDMTAA are shown in figure 2. The corresponding electrochemical parameters' values are extracted using the Stern–Geary equation and are reported in Table 2.

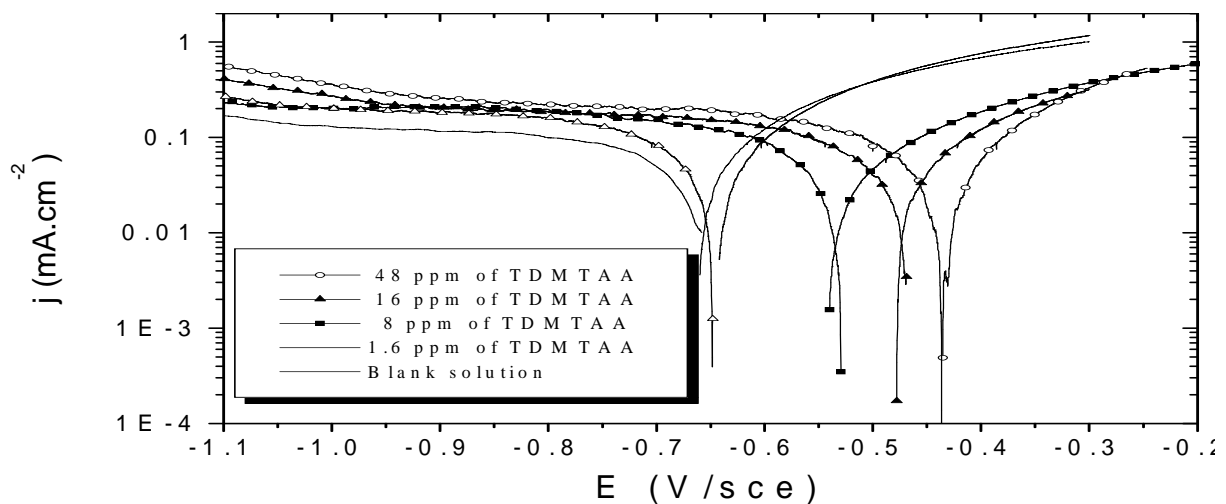


Figure 2: Polarization curves for ordinary steel electrode in cooling water system in presence of different concentration of TDMTAA at 32 °C.

Figure 3 illustrates an example at 8 ppm TDMTAA. We can note that anodic current densities decrease gradually and the potential corrosion (E_{corr}) shifts towards positive values with increasing inhibitor concentration. In the cathodic range, we note an increasing of current plateau with inhibitor. This can be explained by the change of molecules inhibitor orientation which is released from the parts surface metal.

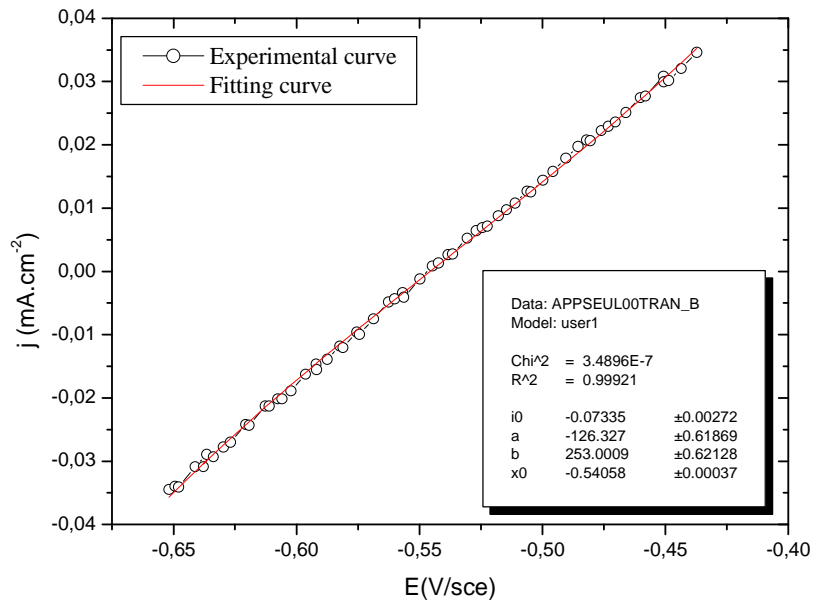


Figure 3: Comparison of experimental and fitting data using a non-linear fitting with Stern–Geary equation (example: 8 ppm for TDMTAA).

The electrochemical parameters extracted from the polarization curves can be depicted from Table 2. These results permitted to conclude that the current densities decrease with increasing inhibitor concentration and reached a maximum at 48 ppm. The approximate constancy of the Tafel slopes (b_a) values indicates that, there is no change in the mechanism of dissolution reaction.

Table 2: Data obtained from polarisation curves of ordinary steel in cooling water system containing different concentration of TDMTAA at 32 °C.

Concentration (ppm)	E_{corr} (mV/sce)	j_{corr} ($\mu A.cm^{-2}$)	b_a (mV/dec)	IE%
00	-661	120	249	-
1.6	-641	100	252	17
8	-540	73	253	39
16	-477	66	248	45
48	-433	55	254	54

Effect of molybdate concentration

The effect of molybdate as a corrosion inhibitor is already well established in the literature [24, 28-33]. The polarization curves for ordinary steel in cooling water system at different concentrations of molybdate are shown in Figure 4. With increasing concentration of Na_2MoO_4 , the corrosion potential obviously shifts positively while the curves shift to lower current densities, which results in a notably decrease in j_{corr} . This figure clearly indicates that ions MoO_3^{2-} act an anodic inhibitor in cooling water system. This can be explained by the adsorption of molybdenum and oxygen ions on the metal surface, leading to the formation of a protective layer with a greater charge transfer resistance and lower

permeability [34, 35]. At the cathodic range, we note that the addition of molybdate ions does not affect the cathodic current density which can be explained, like in the case of TDMTAA, by their orientations.

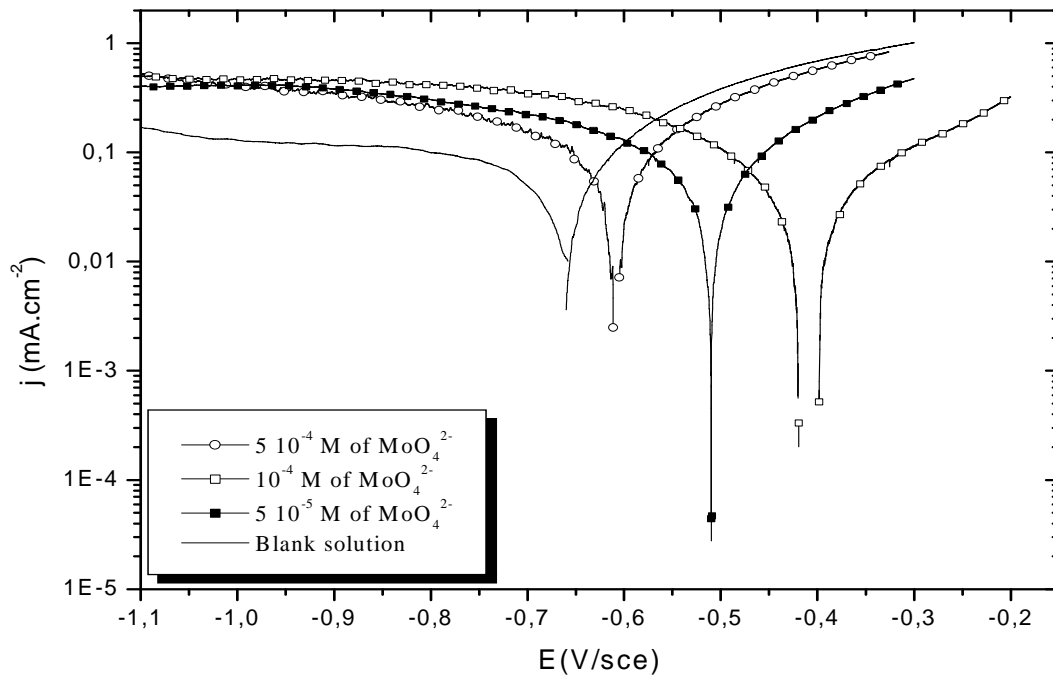


Figure 4: Polarization curves for ordinary steel electrode in the presence of different concentration of MoO_4^{2-} at 32 °C.

Table 3 shows the values of j_{corr} , E_{corr} , Tafel slope (b_a) and percentage inhibition efficiency (IE %) as function of inhibitor concentration. These results permitted to conclude that the current densities decrease with increasing molybdate concentration and the approximate constancy of the b_a values indicate that, there is no change in the mechanism of dissolution reaction in the presence of molybdate. We note that at 10^{-4} M of MoO_4^{2-} ions a marked shift of corrosion potential in the noble direction (marked inhibition).

Table 3: Data obtained from polarisation curves of ordinary steel in cooling water system containing different concentrations of MoO_4^{2-} ions at 32 °C

Concentration (M)	E_{corr} (mV/sce)	j_{corr} ($\mu\text{A}.\text{cm}^{-2}$)	b_a (mV/dec)	IE%
Blank solution	-661	120	249	-
5×10^{-5}	-510	83	255	31
10^{-4}	-400	41	254	66
5×10^{-4}	-605	100	252	17

Effect of mixture inhibitor (TDMTAA + MoO42-)

Figure 5 shows the polarisation curves for ordinary steel in cooling water system at better concentration of the TDMTAA in absence and presence of 10^{-4} M MoO_4^{2-} (mixture) at 32 °C. From these curves, it was found that the corrosive medium reduces the anodic current density markedly without a significant change in the cathodic current density. This behaviour supports that the inhibiting effect of the additive compound increases due to the synergistic effect between the molybdate ions and the used additive. As said before this inhibitor in absence and presence of molybdate ions acts as anodic type inhibitor, therefore only the straight line portion of the anodic branches was considered. The numerical values of electrochemical parameters and inhibition efficiency (IE %) can be depicted from Table 4. These results permitted to conclude that:

- (1) j_{corr} decreases with increasing inhibitor concentration of TDMTAA and more decrease was observed by addition of 10^{-4} M MoO_4^{2-} . This suggests that the molybdate ions have played a role in stabilizing the inhibitor molecules adsorbed on the ordinary steel surface.
- (2) The corrosion potential (E_{corr}) is shifted towards more anodic potential with addition of MoO_4^{2-} .
- (3) The approximate constancy of the Tafel slopes (b_a) values indicates that, there is no change in the mechanism of dissolution reaction.
- (4) The data suggested that TDMTAA acts as anodic type inhibitor in presence or absence of MoO_4^{2-} ions and the decrease in corrosion rate observed during anodic polarization may be attributed to an increase in adsorption.

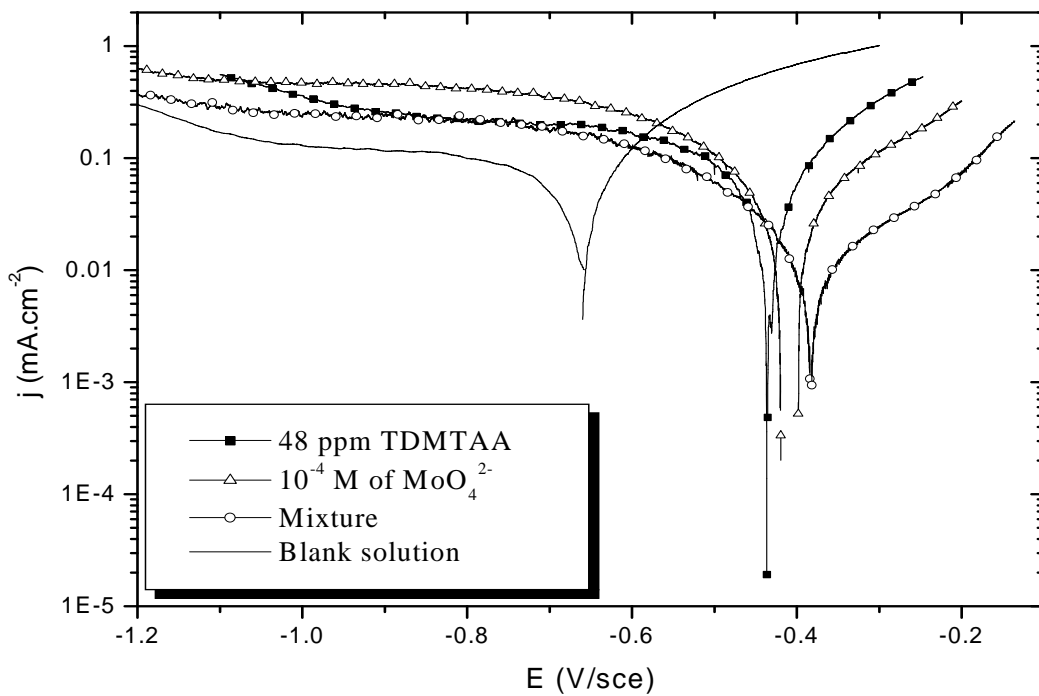


Figure 5. Polarization curves for ordinary steel electrode in the presence of mixture (TDMTAA + 10^{-4} M of MoO_4^{2-}) at 32 °C.

Table 4: Data obtained from polarisation curves of ordinary steel in cooling water system containing different concentration of inhibitors.

	E_{corr} (mV/sce)	j_{corr} ($\mu A.cm^{-2}$)	b_a (mV/dec)	IE%
Blank solution	-661	120	249	-
48 ppm of TDMTAA	-433	55	254	54
10^{-4} M of MoO_4^{2-}	-400	41	254	66
Mixture	-382	12	247	90

Synergism parameter

All the experimental results suggested that addition of $NaMoO_4$ to the inhibited solutions increases the inhibition efficiency and the degree of surface coverage (θ). This behaviour was attributed to the results of synergistic effect between molybdate ions and TDMTAA. For accounting the synergistic effect, Schmitt and Bedhur [35] have proposed two types of joint adsorption namely competitive and cooperative. In competitive adsorption the anion and cation are adsorbed at different sites on the metal surface. In cooperative, the anion is chemisorbed on the surface and the cation is adsorbed on a layer of the anion. The synergism parameter, S_θ , was calculated from the data of polarisation curves techniques using the relationship given by Aramaki and Hackerman [36]:

$$S_{\theta} = \frac{1 - \theta'_{1+2}}{1 - \theta_{1+2}} \tag{3}$$

Where $\theta_{1+2} = \theta_1 + \theta_2 - \theta_1\theta_2$; θ'_{1+2} is the measured surface coverage by both inhibitors; θ_1 , the surface coverage by MoO_4^{2-} and θ_2 is the surface coverage by TDMTAA.

Table 5 gives value of S_{θ} which is more than unity, thereby suggesting that the enhanced inhibition efficiency caused by the addition of molybdate ions to TDMTAA is due to only the synergistic effect. The synergistic inhibition effect in the present work can be explained as follows: The strong chemisorption of molybdate ions on the metal surface is responsible for the synergistic effect of MoO_4^{2-} in combination with the cations of the inhibitor. These cations are then adsorbed by coulombic attraction on the metal surface where molybdate ions are already adsorbed (cooperative adsorption). Stabilization of adsorbed molybdate ions with the inhibitor cations leads to great surface coverage and thereby greater inhibition efficiency.

Table 5: Synergism parameter (S_{θ}) and coverage surface (θ) calculated from polarization measurements.

	E_{corr} (mV/sce)	j_{corr} ($\mu\text{A}\cdot\text{cm}^{-2}$)	b_a (mV/dec)	θ	S_{θ}	IE%
Blank solution	-661	120	249	-	-	-
48 ppm of TDMTAA	-433	55	254	0.5416	-	54
10^{-4}M of MoO_4^{2-}	-400	41	254	0.6583	-	66
Mixture	-382	12	247	0.90	1.56	90

Effect of pH on synergy

In try to examine the effect of mixture (TDMTAA + NaMoO_4) on ordinary steel corrosion in pH range between 4 and 9.5, we have realized polarisation curves measurements. Figure 6 shows the shape of potential-current curves at various pH values. The values of electrochemical parameters are summarised in table 6.

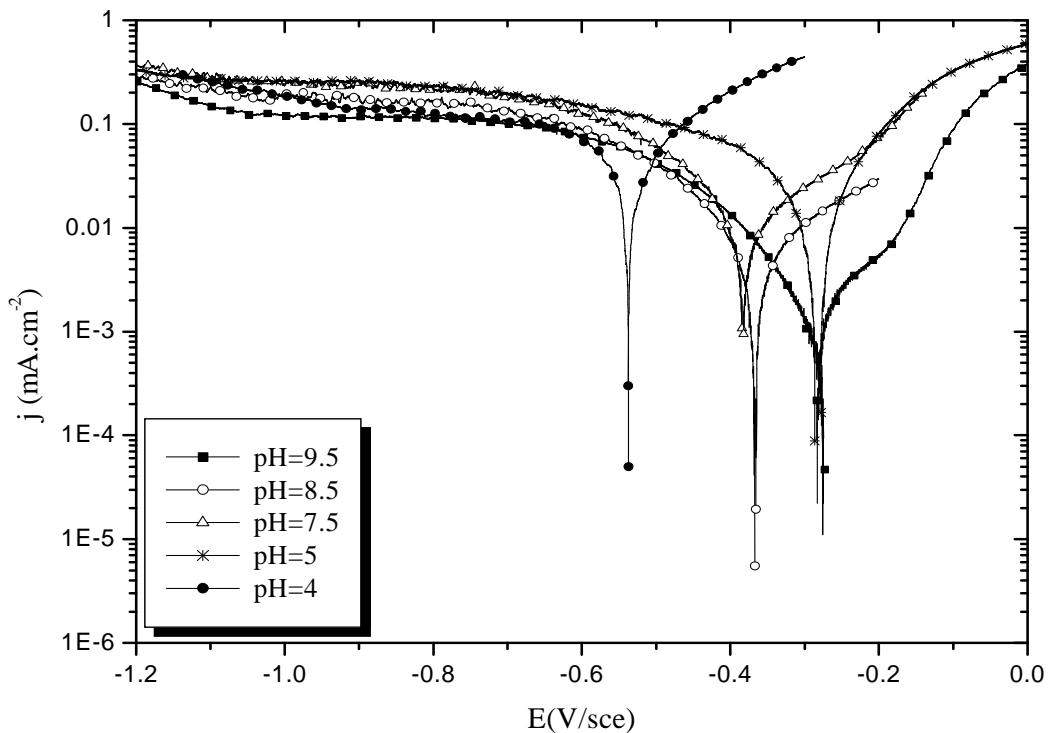


Figure 6: Polarization curves for ordinary steel electrode in the presence of mixture inhibitor in cooling water system at different pH values.

Table 6: Electrochemical parameters of polarization curves of ordinary steel in cooling water system containing mixture of inhibitor at different values pH.

pH	E_{corr} (mV/sce)	j_{corr} ($\mu A.cm^{-2}$)	b_a (mV/dec)	IE%
4	-537	54	234	55
5	-278	32	198	73
7.5	-382	12	247	90
8.5	-365	7	252	94
9.5	-281	2	210	98

We note that the corrosion potential was shifted to anodic values with 252 mV/sce range and the values of j_{corr} decreases from 54 to 2 $\mu A.cm^{-2}$ when the pH increases from 4 to 9.5. According to Sato and al. [37], the passive film on iron in alkaline medium (pH=8.3) has two layers, one is a barrier layer in contact with the metal, and the other a deposit layer, which is formed on the barrier layer. The barrier layer is a Fe^{3+} oxide in the passive potential region and contains a small percentage of Fe^{2+} , while the deposit layer is a hydrated Fe oxide or oxyhydroxide [38,39]. Foley and al. [40] identified by electron diffraction the passive film as $\gamma-Fe_2O_3$ and detected Fe_3O_4 in the active and transpassive regions. The decrease of the passive current could be explained on the basis that dehydration of the hydroxides could occur on the electrode surface during the potential sweep in the noble direction.

In another share, this behaviour can be explained by the fact that the presence of hydroxide ions favours the ionic form of the inhibitors molecules. The ionic form combines with Fe^{2+} to give the corresponding chelate. These results are in perfect agreement with those obtained by Y. Gonzalez and al. which uses aminotrimethyl phosphonic acid (ATMP) as corrosion inhibitor for the carbon steel in 0.1 M NaCl [41].

Effect of temperature on synergy

This effect has been studied with the mixture as best inhibitor using polarisation curves. Corresponding electrochemical parameters are given in table 7.

In the presence of the mixture, we note a decrease of anodic current densities with increasing temperature, and its values are less compared to those obtained with blank solution.

The inhibition efficiency values (IE %) increases with increasing temperature and reaches a value around 95% at range 42-47°C. This result can be explained by the increase of solubility of TDMTAA.

Table 7: Electrochemical parameters of ordinary steel in cooling water system with and without mixture of inhibitor at various temperatures.

	Temperature (K)	E_{corr} (mV/sce)	j_{corr} ($\mu A.cm^{-2}$)	IE%
Blank solution	305	-661	120	-
	310	-671	129	-
	315	-695	151	-
	317	-698	172	-
Mixture	305	-382	12	90
	310	-410	14	89
	315	-377	6	95
	317	-281	7	95

Effect of immersion time on synergy

Figure 7 shows the polarisation curves obtained after different immersion time in cooling water system in the presence of mixture. The evolution of the characteristic parameters with time immersion is summarized in table 8.

We note that the inhibition efficiency increases with increasing immersion time, reaching a maximum after 7h. This result can be explained by the thickening of the film formed (appearance a current plateau for long time). On the basis of the previous electrochemical impedance studies, one can conclude that a gradual replacement of water molecules by the chloride anions and by the adsorption of the inhibitor molecules on the metal surface, decreasing the extent of dissolution reaction [42,43].

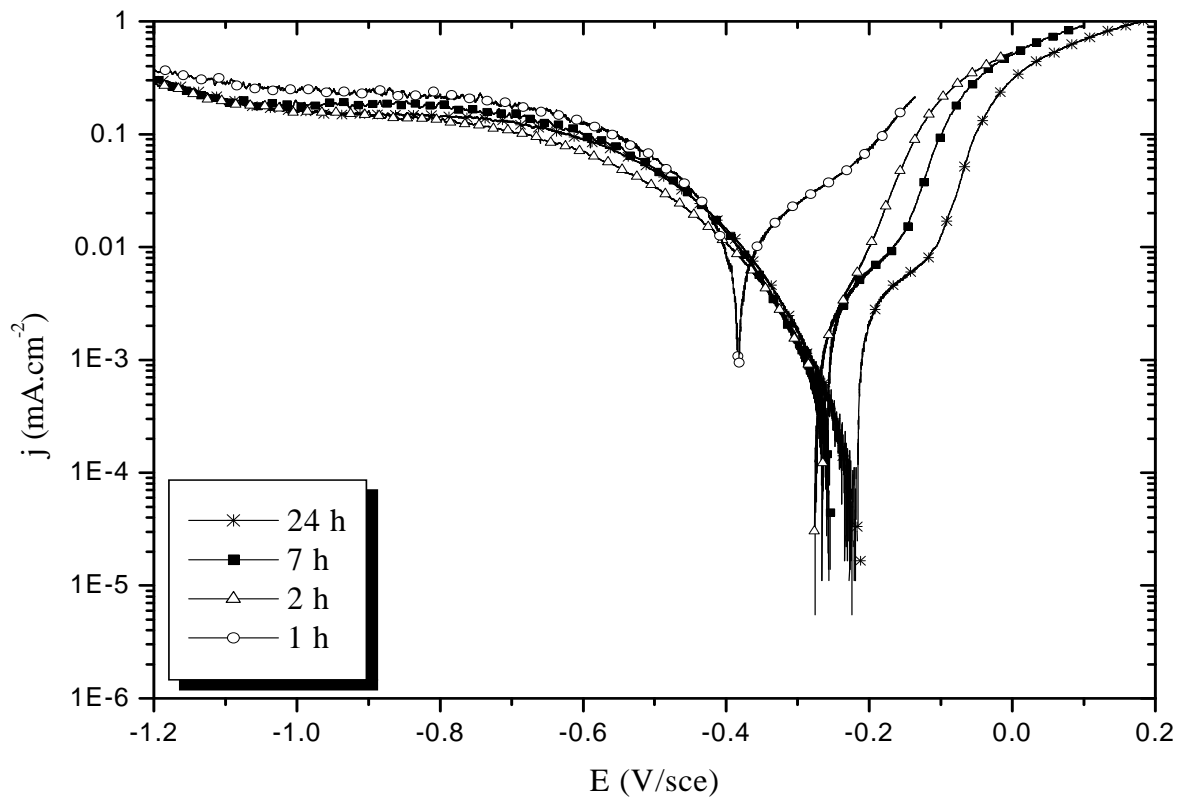


Figure 7. Polarization curves for ordinary steel electrodes in the presence of mixture inhibitor in cooling water system after different immersion times

Table 8: Electrochemical parameters of ordinary steel in cooling water system in the presence of the mixture of inhibitor at various immersion time.

Immersion time (h)	E_{corr} (mV/sce)	j_{corr} ($\mu A.cm^{-2}$)	b_a (mV/dec)	IE%
1	-382	12	247	90
2	-275	3	122	98
7	-258	1	135	99
24	-214	1	137	99

3.2. Scanning electron microscopy (SEM):

Figure 8 shows the scanning electronic microscopy (SEM) images of ordinary steel surface that have been exposed to the cooling water medium for 2 days in the absence and the presence of mixture inhibitors.

The SEM micrograph of the surface exposed to the inhibitor-free solution (figure 8a), shows heterogeneous layer of products. However, an EDX analysis (figure 9.a) further identified characteristic corrosion products elements (Fe, O, S and Cl) as well as the presence of calcium on this layer.

Furthermore, the SEM micrograph of the layer formed in the presence of mixture inhibitors (figure 8b) shows a large area free of corrosion and scale products; hence the presence of very few corrosion products is observed. In this case, EDX analysis (figure 9.b) showed again the presence of calcium and corrosion products, but in very smaller amounts. This indicates that while the mixture inhibitor is a corrosion and scale inhibitor and leads a maximum of 99%.

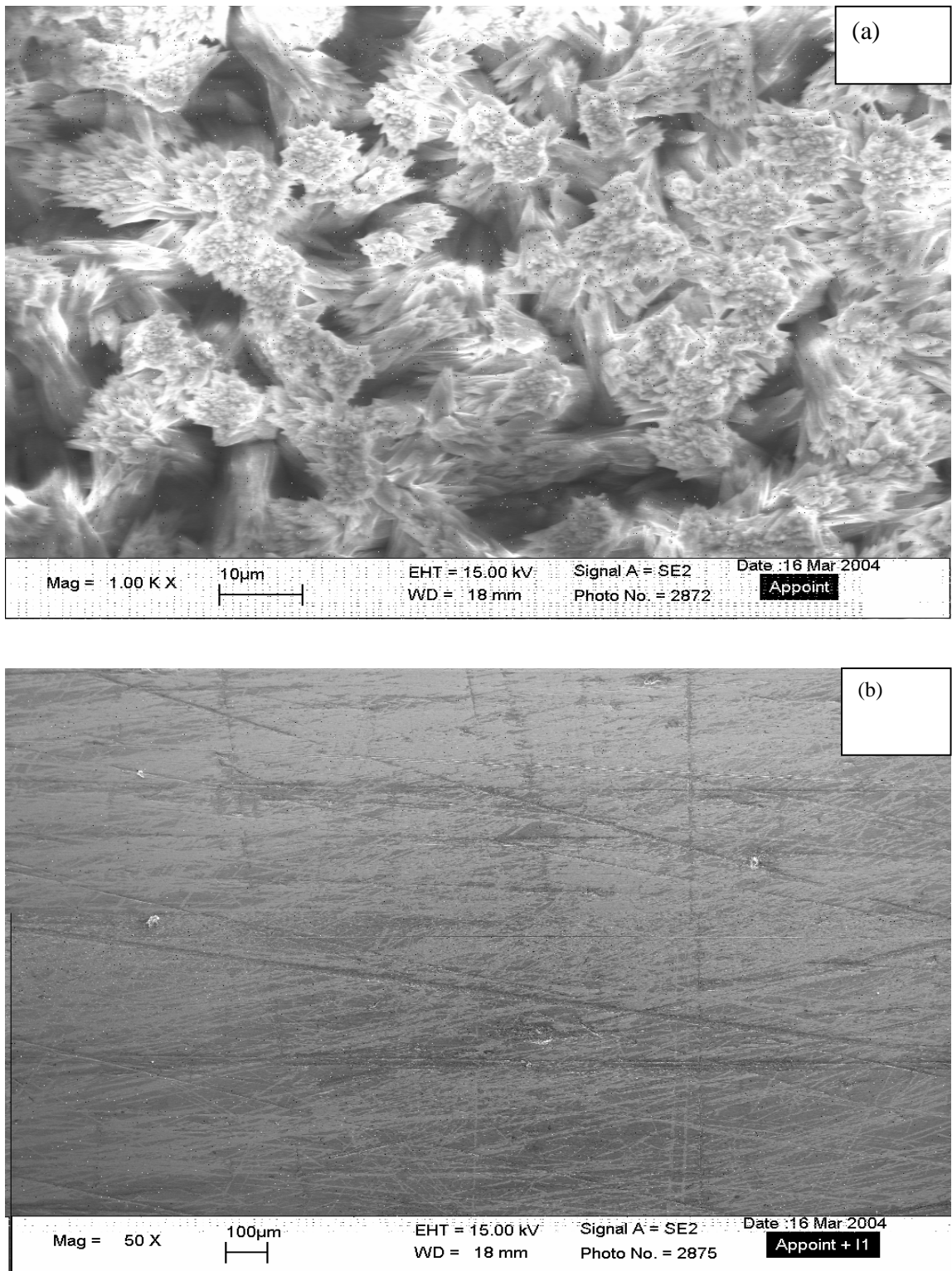


Figure 8: SEM micrographs of ordinary steel surface obtained after 2 days of immersion in the cooling water solution, pH= 7.5 and T=32°C : (a) blank solution (b) with a mixture of inhibitor.

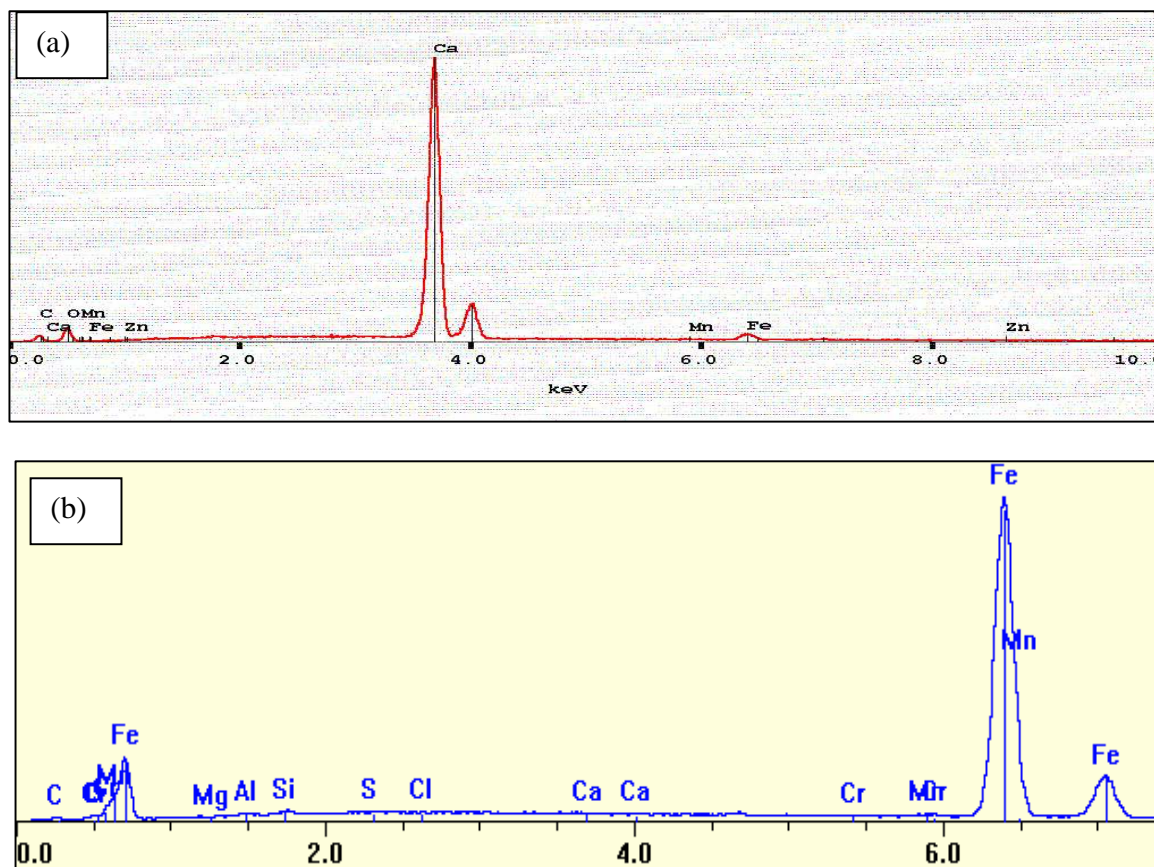


Figure 9: EDX analysis of ordinary steel electrode surface after 2 days immersion in the cooling water solution, pH=7.5 and T=32°C: (a) blank solution (b) with a mixture of inhibitor.

4. Conclusion

The synergistic influence caused by molybdate ions and TDMAA on the inhibition of corrosion and scale of ordinary steel in cooling water system has been studied using polarization curve and scanning electron microscopy (SEM). The addition of molybdate shows a reducing the corrosion rate. The best efficiency (90%) obtained for 10^{-4} M of molybdates ions concentrations and 48 ppm of TDMTAA. The increase in inhibition efficiency in the presence of molybdate ions indicates that MoO_4^{2-} ions enhance the adsorption of TDMTAA on the metal surface. However, the inhibition efficiency of mixture increases by increasing temperature, pH and immersion time.

References

1. Amjad, Z., Butala, D., Pugh, J., The influence of recirculating water impurities on the performance of calcium phosphate inhibiting polymers, Corrosion/99, paper number 118, NACE, Houston, (1999).
2. Puckorius, P.R., Cunningham, B., Cooling water technology advanced course, International water Conference, Pittsburgh, (1997).
3. Sreir, L.L., Jarman, R.A., Corrosion, third ed., Butterworth-Heinemann Ltd., Great Britain, (1994).
4. Banerjee, S.N., An introduction to Science of Corrosion and its Inhibition, Oxonian Press PVT Ltd., India, (1985).
5. Rozenfeld, I.L., Corrosion Inhibition, McGraw-Hill Inc., USA, (1981).

6. Jones, D.A., Principles and Prevention of Corrosion, Macmillan Publishing Company, USA, (1991).
7. Touir, R., Cenoui, M., El Bakri, M., Ebn Touhami, M., *Corros. Sci.*, 50 (2008) 1530.
8. Touir, R., Dkhireche, N., Ebn Touhami, M., Lakhriissi, M., Lakhriissi, B., Sfaira, M., *Desalination*, 249 (2009) 922.
9. Touir, R., Dkhireche, N., Ebn Touhami, M., Sfaira, M., Senhaji, O., Robind, J.J., Boutevind, B., Cherkaoui, M., *Mater. Chem. and Phys.*, 122 (2010) 1.
10. Ochoa, N., Baril, G., Moran F., Pèbère, N., *J. Appl. Electrochem.*, 32 (2002) 497.
11. Marin-Cruz, J., Cabrera-Sierra, R., Pech-Canul, M.A., Gonz´alez, I., *Electrochim. Acta*, 51 (2006) 1847.
12. Ramesh, S., Rajeswari, S., *Electrochim. Acta*, 49 (2004) 811.
13. Choi, D.J., You, S.J., Kim, J.G., *J. Mater. Sci. Engineer.*, A335 (2002) 228.
14. Hinton, BRW., *Met. Finish*, 89 (1991) 55
15. Saremi, M., Dehghanian, C., Mohammadi Sabet, M., *Corros. Sci.*, 48 (2006) 1404.
16. Qing Qu, Lei Li, Shuan Jiang, Wei Bai, Zhongtao Ding, *J Appl. Electrochem.*, 39 (2009) 569.
17. Al-Refaie, A.A., Walton, J., Cottis, R.A., Lindsay, R., *Corros. Sci.*, 52(2010) 422-428
18. Suzuki, F., US Patent 4,176,059, (1979).
19. Robitaille, D.R., Vukasovich, M.S., US Patent 4,138,353, (1979).
20. Lipinski, R.J., US Patent 4,138,353, (1979).
21. Vukasovich, M.S., Sullivan, F.J., US Patent 3,871,089, (1975).
22. Flynn, R.W., Grouke, M.J., US Patent 4,243,316, (1981).
23. Alexander, D.B., Moccari, A.A., *Corrosion*, 49(1993) 921.
24. Kolman, D.G., Taylor, S.R., *Corrosion*, 49 (1993) 622.
25. Chebabe, D., Dermaj, A., Ait Chikh, Z., hajjaji, N., Rico-Lattes, I., Lattes, A., *Synthetic Communications: An International Journal for Rapid Communication of Synthetic Organic Chemistry*, 1532-2432, 34(2004) 4189.
26. Chebabe, D., Ait Chikh, Z., Dermaj, A., Rhattas, K., Jazouli, T., hajjaji, N., El Madari, F., Srhiri, A., *Corros. Sci.*, 46 (2004) 2701.
27. Ait Chikh, Z., Chebabe, D., Dermaj, A., hajjaji, N., Srhiri, A., Montemor, M.F., Ferreira, M.G.S., Bastos, A.C., *Corros. Sci.*, 47 (2005) 447.
28. Farr, J.P.G., Saremi, M., *Surface Technology*, 17 (1982) 19.
29. Farr, J.P.G., Saremi, M., *Surface Technology*, 19 (1983) 137.
30. Bentley, A.J., Saremi, M., *Polyhedron*, 15(1986) 547.
31. Heries, J.J., Bucher, B., *Materials Performance*, 31(1992) 48.
32. Stanick, M.A., *Corrosion*, 40 (1984) 296.
33. Kolman, D.G., Taylor, S.R., *Corrosion*, 49 (1993) 635.
34. Guannan, Mu., Xianghong, Li., Qing, Qu., Zhou, Jun., *Corros. Sci.*, 48 (2006) 445.
35. Schmitt, G., Bedbur, K., *Werkst. Korros.*, 36 (1985) 273.
36. Aramaki, K., Hackerman, N., *J. Electrochem. Soc.*, 116 (1969) 588.
37. Sato, N., Kudo, K., Nishimura, K., *J. Electrochem. Soc.*, 123(1976) 1419.
38. Sato, N., Kudo, K., Noda, T., Z., *Phys. Chem. N.F.*, 98 (1975) 217.
39. Seo, M., Sato, N., Lumsden, J.B., Staehle, R.W., *Corros. Sci.*, 17 (1977) 209.
40. Foley, C.L., Kruger, J., Bechtoldt, C.J., *J. Electrochem. Soc.*, 114 (1967) 994.
41. Gonzalez, Y., Lafont, M.C., Pèbère, N., Moran, F., *J. Appl. Electrochem.*, 26 (1996) 1259.
42. Muralidharam, S., Phani, K.L.N., Pitchumani, S., Ravichadran, S., Lyer, S.V.K., *J. Electrochem. Soc.*, 142 (1995) 1478.
43. Du, T., Chen, J., Cao, D., *J. Mater. Sci.*, 36 (2001) 3903.

(2010) www.jmaterenvironsci.com